Time-dependent transport in interacting and noninteracting resonant-tunneling systems

Antti-Pekka Jauho

*Mikroelektronik Centret, Technical University of Denmark, DK-2800 Lyngby, Denmark,
and Nordita, Blegdamsvej 17, DK-2100 Copenhagen Ø, Denmark*

Ned S. Wingreen

NEC Research Institute, 4 Independence Way, Princeton, New Jersey 08540

Yigal Meir

Department of Physics, University of California at Santa Barbara, Santa Barbara, California 93106
(Received 5 April 1994)

We consider a mesoscopic region coupled to two leads under the influence of external time-dependent voltages. The time dependence is coupled to source and drain contacts, the gates controlling the tunnel-barrier heights, or to the gates that define the mesoscopic region. We derive, with the Keldysh nonequilibrium-Green-function technique, a formal expression for the fully nonlinear, time-dependent current through the system. The analysis admits arbitrary interactions in the mesoscopic region, but the leads are treated as noninteracting. For proportionate coupling to the leads, the time-averaged current is simply the integral between the chemical potentials of the time-averaged density of states, weighted by the coupling to the leads, in close analogy to the time-independent result of Meir and Wingreen [Phys. Rev. Lett. **68**, 2512 (1992)]. Analytical and numerical results for the exactly solvable noninteracting resonant-tunneling system are presented. Due to the coherence between the leads and the resonant site, the current does not follow the driving signal adiabatically: a "ringing" current is found as a response to a voltage pulse, and a complex time dependence results in the case of harmonic driving voltages. We also establish a connection to recent linear-response calculations, and to earlier studies of electron-phonon scattering effects in resonant tunneling.

I. INTRODUCTION

The hallmark of mesoscopic phenomena is the phase coherence of the charge carriers, which is maintained over a significant part of the transport process. The interference effects resulting from this phase coherence are reflected in a number of experimentally measurable properties. For example, phase coherence is central to the Aharonov-Bohm effect,[1] universal conductance fluctuations,[1] and weak localization,[2] and can be affected by external controls such as temperature or magnetic field. The study of stationary mesoscopic physics is now a mature field, and in this work we focus on an alternative way of affecting the phase coherence: external *time-dependent* perturbations. The interplay of external time dependence and phase coherence can be phenomenologically understood as follows. If the single-particle energies acquire a time dependence, then the wave functions have an extra phase factor, $\psi \sim \exp[-i \int^t dt' \epsilon(t')]$. For a uniform system such an overall phase factor is of no consequence. However, if the external time dependence is different in different parts of the system, and the particles can move between these regions (without being "dephased" by inelastic collisions), the phase difference becomes important.

The interest in time-dependent mesoscopic phenomena stems from recent progress in several experimental techniques.[3] Time dependence is a central ingredient in many different experiments, of which we mention the following:

(i) *Single-electron pumps and turnstiles.* Here time-modified gate signals move electrons one by one through a quantum dot, leading to a current which is proportional to the frequency of the external signal. These structures have considerable importance as current standards. The Coulombic repulsion of the carriers in the central region is crucial to the operational principle of these devices, and underlines the fact that extra care must be paid to interactions when considering time-dependent transport in mesoscopic systems.

(ii) ac *response and transients in resonant-tunneling devices.* Resonant-tunneling devices have a number of applications as high-frequency amplifiers or detectors. For the device engineer a natural approach would be to model these circuit elements with resistors, capacitances, and inductors. The question then arises as to what, if any, are the appropriate "quantum" capacitances and inductances one should ascribe to these devices. Answering this question requires the use of time-dependent quantum-transport theory.

(iii) *Interaction with laser fields.* Ultrashort laser pulses allow the study of short-time dynamics of charge carriers. Here again, coherence and time dependence

combine with the necessity of treating interactions.

A rigorous discussion of transport in an interacting mesoscopic system requires a formalism that is capable of including explicitly the interactions. Obvious candidates for such a theoretical tool are various techniques based on Green functions. Since many problems of interest involve systems far from equilibrium, we cannot use linear-response methods, such as those based on the Kubo formula, but must use an approach capable of addressing the full nonequilibrium situation. The nonequilibrum-Green-function techniques, as developed about thirty years ago by Kadanoff and Baym,[4] and by Keldysh,[5] have during the recent years gained increasing attention in the analysis of transport phenomena in mesoscopic semiconductors systems.[6] In particular, the *steady-state* situation has been addressed by a large number of papers.[7−12] Among the central results obtained in these papers is that under certain conditions (to be discussed below) a Landauer-type conductance formula[13] can be derived. This is quite appealing in view of the wide spread success of conductance formulas in the analysis of transport in mesoscopic systems.

Considerably fewer studies have been reported where an explicit time dependence is an essential feature. We are aware of an early paper in surface physics,[14] but only in the recent past have groups working in mesoscopic physics addressed this problem.[15−20,38] The work reported in this paper continues along these lines: we give the full details and expand on our short communication.[17]

Our main formal result from the nonequilibrium-Green-function approach is a general expression for the time-dependent current flowing from noninteracting leads to an interacting region. As we will discuss in Sec. II, the time dependence enters through the self-consistent parameters defining the model. We show that under certain restrictions, to be specified below, a Landauer-like formula can be obtained for the *time-averaged* current. To illustrate the utility of our approach we give results for an exactly solvable noninteracting case, which displays an interesting, and experimentally measurable, nonadiabatic behavior. We also establish a link between the present formulation and recently published results for linear-response and electron-phonon interactions, obtained by other techniques.

The paper is organized as follows. We examine in Sec. II the range of experimental parameters in which we expect our theoretical formulation to be valid. In Sec. III we briefly review the physics behind the nonequilibrium-Green-function technique of Keldysh, and Baym and Kadanoff, which is our main theoretical tool, and then introduce the specific model Hamiltonians used in this work. We derive the central formal results for the time-dependent current in Sec. IV. We also derive, under special restrictions, a Landauer-like formula for the average current. In Sec. V, we apply the general formulas to an explicitly solvable resonant-tunneling model. Both analytical and numerical results are presented. We also show that the linear ac-response results of Fu and Dudley[21] are contained as a special case of the exact results of this section. In Sec. VI, we illustrate the utility of our for-

mulation by presenting a much simplified derivation of Wingreen *et al.*[22] results on resonant tunneling in the presence of electron-phonon interactions. Appendix A summarizes some of the central technical properties of the Keldysh technique: we state the definitions, give the basic equations, and provide the analytic continuation rules employed below. In Appendices B and C, we present proofs for certain statements made in the main text, and, finally, in Appendix D we describe some transformations which facilitate numerical evaluation of the time-dependent current.

II. APPLICABILITY TO EXPERIMENTS

A central question one must address is: under which conditions are the nonequilibrium techniques, applied successfully to the steady-state problem, transferrable to time-dependent situations, such as the experiments mentioned above?

The time-dependent problem has to be formulated carefully, particularly with respect to the leads. It is essential to a Landauer type of approach, that the electrons in the leads be noninteracting. In practice, however, the electrons in the leads near the mesoscopic region contribute to the self-consistent potential. We approach this problem by dividing the transport physics in two steps:[23] (i) the self-consistent determination of charge pileup and depletion in the contacts, the resulting barrier heights, and single-particle energies in the interacting region, and (ii) transport in a system defined by these self-consistent parameters. Step (i) requires a capacitance calculation for each specific geometry,[23] and we do not address it in this paper. Instead, we assume the results of (i) as time-dependent input parameters and give a full treatment of the transport through the mesoscopic region (ii). In practice, the interactions in the leads are absorbed into a time-dependent potential and from then on the electrons in the leads are treated as noninteracting. This means that when relating our results to actual experiments some care must be exercised. Specifically, we calculate only the current flowing into the mesoscopic region, while the total time-dependent current measured in the contacts includes contributions from charge flowing in and out of accumulation and depletion regions in the leads. In the *time-averaged* (dc) current, however, these capacitive contributions vanish and the corresponding time-averaged theoretical formulas, such as Eq. (27), are directly relevant to experiment. It should be noted, though, that these capacitive currents may influence the effective time-dependent parameters in step (i) above.

Let us next estimate the frequency limits that restrict the validity of our approach. Two criteria must be satisfied. First, the driving frequency must be sufficiently slow that the applied bias is dropped entirely across the tunneling structure. When a bias is applied to a sample, the electric field in the leads can only be screened if the driving frequency is smaller than the plasma frequency, which is tens of THz in typical doped semiconductor samples. For signals slower than this, the bias is established entirely across the tunneling structure by accumulation and depletion of charge near the barriers. The unscreened Coulomb interaction between net excess
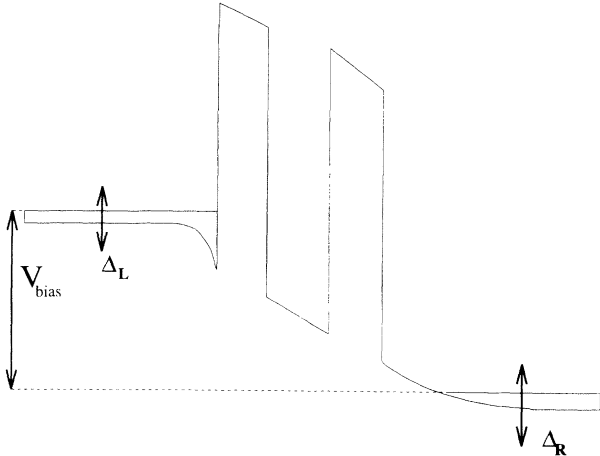
FIG. 1. Sketch of charge distribution in a three dimensional resonant-tunneling device under dc bias $V_{\text{bias}} = \mu_L - \mu_R$ with a time modulation of amplitude $\Delta_{L/R}$ superposed on the leads. As argued in the text, only a tiny fraction of charge carriers participates in setting up the voltage drop across the structure.

charge is quite strong, and hence the bias across a tunneling structure is caused by a relatively small excess of charge in accumulation and depletion layers. The formation of these layers then causes a rigid shift [see Eq. (2) below] of the bottom of the conduction band deeper in the leads, which is the origin of the rigid shift of energy levels in our treatment of a time-dependent bias.

The second frequency limit on our approach is that the buildup of electrons required for the formation of the accumulation and depletion layers must not significantly disrupt the coherent transport of electrons incident from the leads. One way to quantify this is to ask—what is the probability that an electron incident from the leads participates in the buildup of charge associated with a time-dependent bias? This probability will be the ratio of the net current density flowing into the accumulation region to the total incident flux of electrons. For a three-dimensional double-barrier resonant-tunneling structure (see Fig. 1) the ac charging the accumulation layer is $I_{\text{acc}}^{\text{rms}} = 2\pi\nu C V^{\text{rms}}/A$, where ν is the driving frequency, C is the capacitance, V^{rms} is the applied bias, and A is the area. In comparison, the total incident flux is $I_{\text{inc}} = 3/8\,env_F$. Using the parameters appropriate for a typical experiment (we use that of Brown et al.[24]), we find that up to 10 THz the probability of an electron participating in the charge buildup is only 1%. Summarizing, these estimates indicate that our approach should be accurate up to frequencies of tens of THz, which are large by present experimental standards, and consequently the analysis presented in what follows should be valid for most experimental situations.

III. THEORETICAL TOOLS AND THE MODEL

A. Baym-Kadanoff-Keldysh nonequilibrium techniques

Here we wish to outline the physical background behind the Keldysh formulation, and in particular its con-

nection to tunneling physics. Readers interested in technical details should consult any of the many available review articles, such as Refs. 25–27. The basic difference between construction of equilibrium and nonequilibrium perturbation schemes is that in nonequilibrium one cannot assume that the system returns to its ground state (or a thermodynamic equilibrium state at finite temperatures) as $t \to +\infty$. Irreversible effects break the symmetry between $t = -\infty$ and $t = +\infty$, and this symmetry is heavily exploited in the derivation of the equilibrium perturbation expansion. In nonequilibrium situations one can circumvent this problem by allowing the system to evolve from $-\infty$ to the moment of interest (for definiteness, let us call this instant t_0), and then continue the time evolvement from $t = t_0$ back to $t = -\infty$.[28] (When dealing with quantities that depend on two time variables, such as Green functions, the time evolution must be continued to the later time.) The advantage of this procedure is that all expectation values are defined with respect to a well defined state, i.e., the state in which the system was prepared in the remote past. The price is that one must treat the two time branches on an equal footing (See Fig. 2).

A typical object of interest would be a two time Green function (see Appendix A); the two times can be located on either of the two branches of the complex time path (e.g., τ and τ' in Fig. 2). One is thus led to consider 2×2 Green-function matrices, and the various terms in the perturbation theory can be evaluated by matrix multiplication. Since the internal time integrations run over the complex time path, a method of bookkeeping for the time labels is required, and there are various ways of doing this. In the present work we employ a version of the Keldysh technique.

In the context of tunneling problems the time-independent Keldysh formalism works as follows. In the remote past the contacts (i.e., the left and right lead) and the central region are decoupled, and each region is in thermal equilibrium. The equilibrium distribution functions for the three regions are characterized by their respective chemical potentials; these do not have to coincide nor are the differences between the chemical potentials necessarily small. The couplings between the different regions are then established and treated as perturbations via the standard techniques of perturbation theory, albeit on the two-branch time contour. It is important to notice that the couplings do not have to be small, e.g., with respect level spacings or $k_B T$, and typically must be treated to all orders.
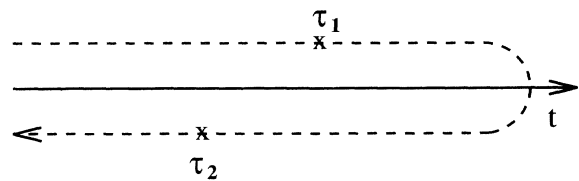

FIG. 2. The complex-time contour on which nonequilibrium-Green-function theory is constructed. In the contour sense, the time τ_1 is earlier than τ_2 even though its real-time projection appears larger.

The time-dependent case can be treated similarly. Before the couplings between the various regions are turned on, the single-particle energies acquire rigid time-dependent shifts, which, in the case of the noninteracting contacts, translate into extra phase factors for the propagators (but not in changes in occupations). The perturbation theory with respect to the couplings has the same diagrammatic structure as in the stationary case. The calculations, of course, become more complicated because of the broken time-translational invariance.

B. Model Hamiltonian

We split the total Hamiltonian in three pieces: $H = H_c + H_T + H_{cen}$, where H_c describes the contacts, H_T is the tunneling coupling between contacts and the interacting region, and H_{cen} models the interacting central region, respectively. Below we discuss each of these terms.

1. Contacts, H_c

Guided by the typical experimental geometry in which the leads rapidly broaden into metallic contacts, we view electrons in the leads as noninteracting except for an overall self-consistent potential. Physically, applying a time-dependent bias between the source and drain contacts corresponds to accumulating or depleting charge to form a dipole around the central region. The resulting electrostatic-potential difference means that the single-particle energies become time dependent: $\epsilon^0_{k\alpha} \rightarrow \epsilon_{k\alpha}(t) = \epsilon^0_{k\alpha} + \Delta_\alpha(t)$ [here α labels the channel in the left (L) or right (R) lead]. The occupation of each state $k\alpha$, however, remains unchanged. The occupation, for each contact, is determined by an equilibrium distribution function established in the distant past, before the time-dependence or tunneling matrix elements are turned on. Thus, the contact Hamiltonian is

$$H_c = \sum_{k,\alpha \in L,R} \epsilon_{k\alpha}(t) c^\dagger_{k\alpha} c_{k\alpha} , \tag{1}$$

and the exact time-dependent Green functions in the leads for the uncoupled system are

$$g^<_{k\alpha}(t,t') \equiv i \langle c^\dagger_{k\alpha}(t') c_{k\alpha}(t) \rangle$$
$$= i f(\epsilon^0_{k\alpha}) \exp\left[-i \int_{t'}^{t} dt_1 \epsilon_{k\alpha}(t_1)\right]$$
$$g^{r,a}_{k\alpha}(t,t') \equiv \mp i\theta(\pm t \mp t') \langle \{c_{k\alpha}(t), c^\dagger_{k\alpha}(t')\} \rangle$$
$$= \mp i\theta(\pm t \mp t') \exp\left[-i \int_{t'}^{t} dt_1 \epsilon_{k\alpha}(t_1)\right] . \tag{2}$$

One should note that our model for $g^<$ differs from the choice made in the recent study of Chen and Ting.[15] The difference does not affect calculations carried out to linear response in the ac drive, but is significant in nonlinear response. Specifically, Chen and Ting allow the electrochemical potential in the distribution function f to vary with time: $\mu_L - \mu_R = e[V + U(t)]$, where $U(t)$ is the ac

signal. This assumption implies that the *total number* of electrons in the contacts varies with time. This behavior is inconsistent with what happens in real devices: it is only the relatively small number of electrons in the accumulation-depletion layers that is time dependent. In addition to the unphysical charge pileup in the contacts, the model of Chen and Ting leads to an instantaneous loss of phase coherence in the contacts, and hence does not display any of the interesting interference phenomena predicted by our phase-conserving model.

2. Coupling between leads and central region, H_T

The coupling between the leads and the central (interacting) region can be modified with time dependent gate voltages, as is the case in single-electron pumps. The precise functional form of the time dependence is determined by the detailed geometry and by the self-consistent response of charge in the contacts to external driving. We assume that these parameters are known, and simply write

$$H_T = \sum_{\substack{k,\alpha \in L,R \\ n}} [V_{k\alpha,n}(t) c^\dagger_{k\alpha} d_n + \text{H.c.}] . \tag{3}$$

Here $\{d^\dagger_n\}$ and $\{d_n\}$ form a complete orthonormal set of single-electron creation and annihilation operators in the interacting region.

3. The central-region Hamiltonian H_{cen}

The form chosen for H_{cen} in the central interacting region depends on geometry and on the physical behavior being investigated. Our results relating the current to local properties, such as densities of states and Green functions, are valid generally. To make the results more concrete, we will discuss two particular examples in detail. In the first, the central region is taken to consist of noninteracting, but time-dependent levels,

$$H_{cen} = \sum_m \epsilon_m(t) d^\dagger_m d_m. \tag{4}$$

Here $d^\dagger_m$ (d_m) creates (destroys) an electron in state m. The choice (4) represents a simple model for time-dependent resonant tunneling. Below we shall present general results for an arbitrary number of levels, and analyze the case of a single level in detail. The latter is interesting both as an exactly solvable example, and for predictions of coherence effects in time-dependent experiments.

The second example we will discuss is resonant tunneling with electron-phonon interaction,

$$H^{el-ph}_{cen} = \epsilon_0 d^\dagger d + d^\dagger d \sum_q M_q [a^\dagger_q + a_{-q}] . \tag{5}$$

In the above, the first term represents a single site, while the second term represents the interaction of an electron on the site with phonons: $a^\dagger_q (a_q)$ creates (destroys) a phonon in mode q, and M_q is the interaction matrix element. The full Hamiltonian of the system

must also include the free-phonon contribution $H_{\rm ph} = \sum_q \hbar\omega_q a_q^\dagger a_q$. This example, while not exactly solvable, is helpful to show how interactions influence the current. Furthermore, we can directly compare to previous time-independent results[22] using (5) to demonstrate the power of the present formalism.

IV. TIME-DEPENDENT CURRENT AND KELDYSH GREEN FUNCTIONS

A. General expression for the current

The current from the left contact through the left barrier to the central region can be calculated from the time evolution of the occupation number operator of the left contact:

$$J_L(t) = -e\langle \dot{N}_L \rangle = -\frac{ie}{\hbar}\langle [H, N_L] \rangle , \qquad (6)$$

where $N_L = \sum_{k,\alpha\in L} c_{k\alpha}^\dagger c_{k\alpha}$ and $H = H_c + H_T + H_{\rm cen}$. Since H_c and $H_{\rm cen}$ commute with N_L, one readily finds

$$J_L = \frac{ie}{\hbar} \sum_{\substack{k,\alpha\in L \\ n}} [V_{k\alpha,n}\langle c_{k\alpha}^\dagger d_n \rangle - V_{k\alpha,n}^*\langle d_n^\dagger c_{k\alpha} \rangle] . \qquad (7)$$

Now define two Green functions

$$G_{n,k\alpha}^<(t,t') \equiv i\langle c_{k\alpha}^\dagger(t') d_n(t) \rangle, \qquad (8)$$

$$G_{k\alpha,n}^<(t,t') \equiv i\langle d_n^\dagger(t') c_{k\alpha}(t) \rangle . \qquad (9)$$

Using $G_{k\alpha,n}^<(t,t) = -\left[G_{n,k\alpha}^<(t,t)\right]^*$, and inserting the time labels, the current can be expressed as

$$J_L(t) = \frac{2e}{\hbar}\mathrm{Re}\left\{ \sum_{\substack{k,\alpha\in L \\ n}} V_{k\alpha,n}(t) G_{n,k\alpha}^<(t,t) \right\} . \qquad (10)$$

One next needs an expression for $G_{n,k\alpha}^<(t,t')$. For the present case, with noninteracting leads, a general relation for the contour-ordered Green function $G_{n,k\alpha}(\tau,\tau')$ can be derived rather easily (either with the equation-of-motion technique, or by a direct expansion of the S matrix; the details are given in Appendix B), and the result is

$$G_{n,k\alpha}(\tau,\tau') = \sum_m \int d\tau_1 G_{nm}(\tau,\tau_1)$$

$$\times V_{k\alpha,m}^*(\tau_1) g_{k\alpha}(\tau_1,\tau') . \qquad (11)$$

Here $G_{nm}(\tau,\tau_1)$ is the contour-ordered Green function for the central region, and the τ variables are now defined on the contour of Fig. 2. Note that the time dependence of the tunneling matrix elements and single-particle energies has broken the time-translational invariance. The analytic continuation rules (A3) of Appendix A can now be applied, and we find

$$G_{n,k\alpha}^<(t,t') = \sum_m \int dt_1 V_{k\alpha,m}^*(t_1)$$

$$\times [G_{nm}^r(t,t_1) g_{k\alpha}^<(t_1,t') + G_{nm}^<(t,t_1) g_{k\alpha}^a(t_1,t')] , \qquad (12)$$

where the Green functions $g^{<,a}$ for the leads are defined in (2) above. Combining (2), (10), and (12), yields

$$J_L(t) = -\frac{2e}{\hbar}\mathrm{Im}\left\{ \sum_{\substack{k,\alpha\in L \\ n,m}} V_{k\alpha,n}(t) \int_{-\infty}^t dt_1 \right.$$

$$\times e^{i\int_{t_1}^t dt_2 \epsilon_{k\alpha}(t_2)} V_{k\alpha,m}^*(t_1)$$

$$\left. \times [G_{nm}^r(t,t_1) f_L(\epsilon_{k\alpha}) + G_{nm}^<(t,t_1)] \right\} . \qquad (13)$$

The discrete sum over k in $\sum_{k\alpha}$ can be expressed in terms of densities of states in the leads: $\int d\epsilon \rho_\alpha(\epsilon)$. Then it is useful to define

$$\left[\Gamma^L(\epsilon,t_1,t)\right]_{mn} = 2\pi \sum_{\alpha\in L} \rho_\alpha(\epsilon) V_{\alpha,n}(\epsilon,t) V_{\alpha,m}^*(\epsilon,t_1)$$

$$\times \exp\left[i\int_{t_1}^t dt_2 \Delta_\alpha(\epsilon,t_2)\right] , \qquad (14)$$

where $V_{k\alpha,n} = V_{\alpha,n}(\epsilon_k)$. In terms of this generalized linewidth function (14), the general expression for the current is

$$J_L(t) = -\frac{2e}{\hbar} \int_{-\infty}^t dt_1 \int \frac{d\epsilon}{2\pi}\mathrm{Im}\mathrm{Tr}\left\{ e^{-i\epsilon(t_1-t)}\Gamma^L(\epsilon,t_1,t) \right.$$

$$\left. \times [\mathbf{G}^<(t,t_1) + f_L(\epsilon)\mathbf{G}^r(t,t_1)] \right\} . \qquad (15)$$

Here the boldface notation indicates that the level-width function Γ and the central-region Green functions $\mathbf{G}^{<,r}$ are matrices in the central-region indeces m, n. An analogous formula applies for $J_R(t)$, the current flowing into the central region through the right barrier.

This is the central formal result of this work, and the remainder of this paper is devoted to the analysis and evaluation of Eq. (15). The current is expressed in terms of local quantities: Green functions of the central region. The first term in Eq. (15), which is proportional to the lesser function $G^<$, suggests an interpretation as the out-tunneling rate [recalling $\mathrm{Im}\,G^<(t,t) = N(t)$]. Likewise, the second term, which is proportional to the occupation in the leads and to the density of states in the central region, can be associated to the in-tunneling rate. However, one should bear in mind that all Green functions in Eq. (15) are to be calculated in the presence of tunneling. Thus, $G^<$ will depend on the occupation in the leads. Furthermore, in the presence of interactions G^r will depend on the central-region occupation. Consequently, the current can be a nonlinear function of the occupation factors. This issue has recently been discussed also by other authors.[29]

B. Time-independent case

1. General expression

In the time-independent limit the linewidth function simplifies: $\Gamma(\epsilon, t_1, t) \to \Gamma(\epsilon)$, and the t_1 integrals in Eq. (15) can be performed:

$$\int_{-\infty}^{t} dt_1 \int \frac{d\epsilon}{2\pi} \mathrm{Im\,Tr}\Big\{ e^{-i\epsilon(t_1-t)}\Gamma^L(\epsilon)\mathbf{G}^<(t-t_1) \Big\}$$

$$= -\frac{i}{2}\int \frac{d\epsilon}{2\pi}\mathrm{Tr}\{\Gamma^L(\epsilon)\mathbf{G}^<(\epsilon)\} , \quad (16)$$

and

$$\int_{-\infty}^{t} dt_1 \int \frac{d\epsilon}{2\pi} \mathrm{Im\,Tr}\Big\{ e^{-i\epsilon(t_1-t)}\Gamma^L(\epsilon)f_L(\epsilon)\mathbf{G}^r(t-t_1) \Big\}$$

$$= -\frac{i}{2}\int \frac{d\epsilon}{2\pi}\mathrm{Tr}\Big\{ \Gamma^L(\epsilon)f_L(\epsilon)\big[\mathbf{G}^r(\epsilon) - \mathbf{G}^a(\epsilon)\big] \Big\} . \quad (17)$$

When these expressions are substituted to Eq. (15), the current from the left (right) contact to the central region becomes

$$J_{L(R)} = \frac{ie}{\hbar}\int \frac{d\epsilon}{2\pi}\mathrm{Tr}\Big\{ \Gamma^{L(R)}(\epsilon)\big(\mathbf{G}^<(\epsilon)$$

$$+ f_{L(R)}(\epsilon)[\mathbf{G}^r(\epsilon) - \mathbf{G}^a(\epsilon)]\big) \Big\} . \quad (18)$$

In steady state, the current will be uniform, so that $J = J_L = -J_R$, and one can symmetrize the current: $J = (J_L + J_L)/2 = (J_L - J_R)/2$. Using Eq. (18) leads to the general expression for the dc current:

$$J = \frac{ie}{2\hbar}\int \frac{d\epsilon}{2\pi}\mathrm{Tr}\Big\{ [\Gamma^L(\epsilon) - \Gamma^R(\epsilon)]\mathbf{G}^<(\epsilon)$$

$$+ [f_L(\epsilon)\Gamma^L(\epsilon) - f_R(\epsilon)\Gamma^R(\epsilon)][\mathbf{G}^r(\epsilon) - \mathbf{G}^a(\epsilon)] \Big\} . \quad (19)$$

This result was reported in Ref. 7, and applied to the out-of-equilibrium Anderson impurity problem.

2. Proportionate coupling

If the left and right linewidth functions are proportional to each other, i.e., $\Gamma^L(\epsilon) = \lambda\Gamma^R(\epsilon)$, further simplification can be achieved. We observe that the current can be written as $J \equiv xJ_L - (1-x)J_R$, which gives, using Eq. (18),

$$J = \frac{ie}{\hbar}\int \frac{d\epsilon}{2\pi}\mathrm{Tr}\Big\{ \Gamma^R(\epsilon)\big[(\lambda x - (1-x))\mathbf{G}^<(\epsilon)$$

$$+ (\lambda x f_L - (1-x)f_R)(\mathbf{G}^r(\epsilon) - \mathbf{G}^a)(\epsilon)\big] \Big\} . \quad (20)$$

The arbitrary parameter x is now fixed so that the first term vanishes, i.e., $x = 1/(1 + \lambda)$, which results in

$$J = \frac{ie}{\hbar}\int \frac{d\epsilon}{2\pi}[f_L(\epsilon) - f_R(\epsilon)]$$

$$\times \mathrm{Tr}\Big\{ \frac{\Gamma^L(\epsilon)\Gamma^R(\epsilon)}{\Gamma^L(\epsilon) + \Gamma^R(\epsilon)}[\mathbf{G}^r(\epsilon) - \mathbf{G}^a(\epsilon)] \Big\} . \quad (21)$$

The ratio is well defined because the Γ matrices are proportional. The difference between the retarded and advanced Green functions is essentially the density of states. Despite the apparent similarity of (21) to the Landauer formula, it is important to bear in mind that in general there is no immediate connection between the quantity

$$\mathrm{Tr}\Big\{ \big(\Gamma^L(\epsilon)\Gamma^R(\epsilon)/[\Gamma^L(\epsilon) + \Gamma^R(\epsilon)]\big)[\mathbf{G}^r(\epsilon) - \mathbf{G}^a(\epsilon)] \Big\},$$

and the transmission coefficient. In particular, when inelastic scattering is present, we do not believe that such a connection exists. In Sec. V, where we analyze a noninteracting central region, a connection with the transmission coefficient can be established. Further, in the next section we shall see how an analogous result can be derived for the average of the time-dependent current.

C. Average current

In analogy with the previous subsection, where we found a compact expression for the current for the case of proportionate coupling, the time-dependent case allows further simplification, if assumptions are made on the linewidth functions. In this case, we assume a generalized proportionality condition

$$\Gamma^L(\epsilon, t_1, t) = \lambda\Gamma^R(\epsilon, t_1, t) . \quad (22)$$

One should note that in general this condition can be satisfied only if $\Delta_\alpha^L(t) = \Delta_\alpha^R(t) = \Delta(t)$. However, in the wide-band limit (WBL), to be considered in detail below, the time variations of the energies in the leads do not have to be equal.

We next consider the occupation of the central region $N(t) = \sum_m \langle d_m^\dagger(t)d_m(t)\rangle$ and apply the continuity equation

$$e\frac{dN(t)}{dt} = J_R(t) + J_L(t) , \quad (23)$$

which allows one to write for arbitrary x

$$J_L(t) = xJ_L(t) + (1-x)\left[e\frac{dN(t)}{dt} - J_R(t)\right] . \quad (24)$$

Choosing now $x \equiv 1/(1 + \lambda)$ leads to

$$J_L(t) = \left(\frac{\lambda}{1+\lambda}\right)\left[e\frac{dN}{dt} - \frac{2e}{\hbar}\mathrm{Im\,Tr}\Big\{ \int_{-\infty}^{t} dt_1 \int \frac{d\epsilon}{2\pi}\right.$$

$$\times e^{-i\epsilon(t_1-t)}\Gamma^R(\epsilon, t_1, t)\mathbf{G}^r(t, t_1)$$

$$\left.\times [f_L(\epsilon) - f_R(\epsilon)]\Big\} \right] . \quad (25)$$

The time average of a time-dependent object $F(t)$ is defined by

$$\langle F(t) \rangle = \lim_{T \to \infty} \frac{1}{T} \int_{-T/2}^{T/2} dt \, F(t) \, . \qquad (26)$$

If $F(t)$ is a periodic function of time, it is sufficient to average over the period. Upon time averaging, the first term in Eq. (25) vanishes, $\langle dN/dt \rangle \to 0$, because the occupation $N(t)$ is finite for all T. The expression for the time-averaged current further simplifies if one can factorize the energy and time dependence of the tunneling coupling, $V_{k\alpha,n}(t) \equiv u(t)V_{\alpha,n}(\epsilon_k)$. We then obtain

$$\langle J_L(t) \rangle = -\frac{2e}{\hbar} \int \frac{d\epsilon}{2\pi} [f_L(\epsilon) - f_R(\epsilon)]$$
$$\times \mathrm{Im}\mathrm{Tr}\left\{ \frac{\boldsymbol{\Gamma}^L(\epsilon)\boldsymbol{\Gamma}^R(\epsilon)}{\boldsymbol{\Gamma}^L(\epsilon) + \boldsymbol{\Gamma}^R(\epsilon)} \langle u(t)\mathbf{A}(\epsilon,t) \rangle \right\} \, , \quad (27)$$

where

$$\mathbf{A}(\epsilon,t) = \int dt_1 u(t_1)\mathbf{G}^r(t,t_1)$$
$$\times \exp\left[i\epsilon(t-t_1) + i\int_{t_1}^{t} dt_2 \Delta(t_2) \right] \, . \qquad (28)$$

Due to Eq. (22) we do not have to distinguish between L/R in the definition of $\mathbf{A}(\epsilon,t)$; below we shall encounter situations where this distinction is necessary.

The expression (27) is of the Landauer type: it expresses the current as an integral over a weighted density

of states times the difference of the two contact occupation factors. It is valid for arbitrary interactions in the central region, but it was derived with the somewhat restrictive assumption of proportional couplings to the leads.

V. NONINTERACTING RESONANT-LEVEL MODEL

A. General formulation

In the noninteracting case the Hamiltonian is $H = H_c + H_T + H_{\mathrm{cen}}$, where $H_{\mathrm{cen}} = \sum_n \epsilon_n d_n^\dagger d_n$. Following standard analysis (an analogous calculation is also carried out in Appendix B), one can derive the Dyson equation for the retarded Green function,

$$\mathbf{G}^r(t,t') = \mathbf{g}^r(t,t') + \int dt_1 \int dt_2 \mathbf{g}^r(t,t_1)$$
$$\times \boldsymbol{\Sigma}^r(t_1,t_2)\mathbf{G}^r(t_2,t') \, , \qquad (29)$$

where

$$\Sigma_{nn'}^r(t_1,t_2) = \sum_{k\alpha \in L,R} V_{k\alpha,n}^*(t_1)g_{k\alpha}^r(t_1,t_2)$$
$$\times V_{k\alpha,n'}(t_2) \, , \qquad (30)$$

and $g_{k\alpha}^r$ is given by Eq. (2). From (A4) the Keldysh equation for $G^<$ is[30]

$$\mathbf{G}^<(t,t') = \int dt_1 \int dt_2 \mathbf{G}^r(t,t_1)\boldsymbol{\Sigma}^<(t_1,t_2)\mathbf{G}^a(t_2,t')$$

$$= i \int dt_1 \int dt_2 \mathbf{G}^r(t,t_1)\left[\sum_{L,R} \int \frac{d\epsilon}{2\pi} e^{-i\epsilon(t_1-t_2)} f_{L/R}(\epsilon)\boldsymbol{\Gamma}^{L/R}(\epsilon,t_1,t_2) \right] \mathbf{G}^a(t_2,t') \, . \qquad (31)$$

Provided that the Dyson equation for the retarded Green function can be solved, Eq. (31) together with the current expression Eq. (15) provides the complete solution to the noninteracting resonant-level model. Below we examine special cases where analytic progress can be made.

B. Time-independent case

In the time-independent case the time-translational invariance is restored, and it is advantageous to go over to energy variables

$$\mathbf{G}^r(\epsilon) = [(\mathbf{g}^r)^{-1} - \boldsymbol{\Sigma}^r(\epsilon)]^{-1}$$
$$\mathbf{G}^<(\epsilon) = \mathbf{G}^r(\epsilon)\boldsymbol{\Sigma}^<(\epsilon)\mathbf{G}^a(\epsilon) \, . \qquad (32)$$

In general, the Dyson equation for the retarded Green function requires matrix inversion. In the case of a single level, the scalar equations can be readily solved. The retarded (advanced) self-energy is

$$\Sigma^{r,a}(\epsilon) = \sum_{k\alpha \in L,R} \frac{|V_{k\alpha}|^2}{\epsilon - \epsilon_{k\alpha} \pm i\eta} = \Lambda(\epsilon) \mp \frac{i}{2}\Gamma(\epsilon) \, , \quad (33)$$

where the real and imaginary parts contain "left" and "right" contributions: $\Lambda(\epsilon) = \Lambda^L(\epsilon) + \Lambda^R(\epsilon)$ and $\Gamma(\epsilon) = \Gamma^L(\epsilon) + \Gamma^R(\epsilon)$. The lesser self-energy is

$$\Sigma^<(\epsilon) = \sum_{k\alpha \in L,R} |V_{k\alpha}|^2 g_{k\alpha}^<(\epsilon)$$
$$= i[\Gamma^L(\epsilon)f_L(\epsilon) + \Gamma^R(\epsilon)f_R(\epsilon)] \, . \qquad (34)$$

Using the identities $G^r G^a = (G^r - G^a)/(1/G^a - 1/G^r) = a(\epsilon)/\Gamma(\epsilon)$ {here $a(\epsilon) = i[G^r(\epsilon) - G^a(\epsilon)]$ is the spectral function}, one can write $G^<$ in a "pseudoequilibrium" form

$$G^<(\epsilon) = ia(\epsilon)\bar{f}(\epsilon) \, , \qquad (35)$$

where

$$\bar{f}(\epsilon) = \frac{\Gamma^L(\epsilon)f_L(\epsilon) + \Gamma^R(\epsilon)f_R(\epsilon)}{\Gamma(\epsilon)},$$

$$a(\epsilon) = \frac{\Gamma(\epsilon)}{[\epsilon - \epsilon_0 - \Lambda(\epsilon)]^2 + [\Gamma(\epsilon)/2]^2} \cdot \quad (36)$$

With these expressions the evaluation of the current (19) is straightforward

$$J = -\frac{e}{2\hbar} \int \frac{d\epsilon}{2\pi} a(\epsilon) \left\{ [\Gamma^L(\epsilon) - \Gamma^R(\epsilon)]\bar{f}(\epsilon) \right.$$
$$\left. - [f_L(\epsilon)\Gamma^L(\epsilon) - f_R(\epsilon)\Gamma^R)] \right\}$$

$$= \frac{e}{\hbar} \int \frac{d\epsilon}{2\pi} \frac{\Gamma^L(\epsilon)\Gamma^R(\epsilon)}{[\epsilon - \epsilon_0 - \Lambda(\epsilon)]^2 + [\Gamma(\epsilon)/2]^2}$$
$$\times [f_L(\epsilon) - f_R(\epsilon)] . \quad (37)$$

Note that this derivation made no assumptions about proportionate coupling to the leads. The factor multiplying the difference of the Fermi functions is the elastic transmission coefficient. It is important to understand the difference between this result and the result obtained in Sec. III B 2 (despite the similarity of appearance): There Eq. (21) gives the current for a fully interacting system, and the evaluation of the retarded and advanced Green functions requires a consideration of interactions (e.g., electron-electron, electron-phonon, and spin-flip) in addition to tunneling back and forth to the contacts. *Suppose* now that the Green function for the interacting central region can be solved, $G^{r,a}(\epsilon) = [\epsilon - \epsilon_0 - \lambda(\epsilon) \pm i\gamma(\epsilon)/2]^{-1}$, where λ and $\gamma/2$ are the real and imaginary parts of the self-energy (including interactions *and* tunneling). Then the interacting result for proportionate coupling (21) becomes

$$J = \frac{e}{\hbar} \int \frac{d\epsilon}{2\pi} [f_L(\epsilon) - f_R(\epsilon)] \frac{\Gamma^L(\epsilon)\Gamma^R(\epsilon)}{\Gamma^L(\epsilon) + \Gamma^R(\epsilon)}$$
$$\times \frac{\gamma(\epsilon)}{[\epsilon - \epsilon_0 - \lambda(\epsilon)]^2 + [\gamma(\epsilon)/2]^2} \cdot \quad (38)$$

This result coincides with the noninteracting current expression (37) if $\lambda(\epsilon) \to \Lambda(\epsilon)$ and $\gamma(\epsilon) \to \Gamma(\epsilon) = \Gamma^R(\epsilon) + \Gamma^L(\epsilon)$. In a phenomenological model, where the total level width is expressed as a sum of elastic and inelastic widths, $\gamma = \gamma_e + \gamma_i$, one recovers the results of Jonson and Grincwajg, and Weil and Vinter.[31]

C. Wide-band limit

1. Basic formulas

For simplicity, we continue to consider only a single level in the central region. As in the previous section, we assume that one can factorize the momentum and time dependence of the tunneling coupling, but allow for different time dependence for each barrier: $V_{k\alpha}(t) \equiv u_{L/R}(t)V_{\alpha,n}(\epsilon_k)$. Referring to Eq. (33), the wide-band limit consists of (i) neglecting the level shift $\Lambda(\epsilon)$, (ii) assuming that the linewidths are energy independent con-

stants, $\sum_{\alpha \in L,R} \Gamma_\alpha = \Gamma^{L/R}$, and (iii) allowing a single time dependence, $\Delta_{L/R}(t)$, for the energies in each lead.

Let us comment on the relevance of the WBL. This approximation captures the main physics in a range of applications, and has the great advantage of yielding explicit analytic results. In particular, transport is often dominated by states close to the Fermi level, and since $\Gamma(\epsilon)$ and $\Lambda(\epsilon)$ are generally slowly varying functions of energy, the WBL for this case is an excellent approximation. The WBL also allows asymmetric barriers ($\Gamma_L \neq \Gamma_R$). Consequently, it is possible to describe resonant-tunneling systems under high bias by using a suitable model for the bias dependence of the level widths and/or shifts. Finally, while the simplest WBL leads to an unphysical monotonic *I-V* curve for a resonant-tunneling diode (because the model lacks band edges), it is relatively simple to generalize the WBL so that it does yield negative differential resistance, see Sec. IV C 4 below.

The retarded self-energy in Eq. (29) thus becomes

$$\Sigma^r(t_1, t_2) = \sum_{\alpha \in L,R} u_\alpha^*(t_1)u_\alpha(t_2)e^{-i\int_{t_2}^{t_1} dt_3 \Delta_\alpha(t_3)}$$

$$\times \int \frac{d\epsilon}{2\pi} e^{-i\epsilon(t_1 - t_2)} \theta(t_1 - t_2)[-i\Gamma_\alpha]$$

$$= -\frac{i}{2}[\Gamma^L(t_1) + \Gamma^R(t_1)]\delta(t_1 - t_2) . \quad (39)$$

(Here we have introduced the notation $\Gamma^{L/R}(t_1) \equiv \Gamma^{L/R}(t_1, t_1) = \Gamma^{L/R}|u_{L/R}(t_1)|^2$.) With this self-energy, the retarded (advanced) Green function becomes[16,22]

$$G^{r,a}(t, t') = g^{r,a}(t, t') \exp\left\{ \mp \int_{t'}^{t} dt_1 \frac{1}{2}[\Gamma^L(t_1) \right.$$
$$\left. + \Gamma^R(t_1)] \right\} \quad (40)$$

with

$$g^{r,a}(t, t') = \mp i\theta(\pm t \mp t')$$
$$\times \exp\left[-i \int_{t'}^{t} dt_1 \epsilon_0(t_1) \right] . \quad (41)$$

This solution can now be used to evaluate the lesser function Eq. (31), and further in Eq. (15), to obtain the time-dependent current. In the WBL the ϵ and t_1 integrals in the term involving $G^<$ are readily evaluated, and we write the current as [using Im$\{G^<(t,t)\} = N(t)$, where $N(t)$ is the occupation of the resonant level]

$$J_L(t) = -\frac{e}{\hbar} \left[\Gamma^L(t)N(t) + \int \frac{d\epsilon}{\pi} f_L(\epsilon) \right.$$

$$\times \int_{-\infty}^{t} dt_1 \Gamma^L(t_1, t)$$

$$\left. \times \text{Im}\{ e^{-i\epsilon(t_1 - t)} G^r(t, t_1) \} \right] . \quad (42)$$

For a compact notation we introduce

$$A_{L/R}(\epsilon, t) = \int dt_1 u_{L/R}(t_1) G^r(t, t_1)$$

$$\times \exp\left[i\epsilon(t - t_1) - i \int_t^{t_1} dt_2 \Delta_{L/R}(t_2)\right] .$$

$$(43)$$

Obviously, in the time-independent case $A(\epsilon)$ is just the Fourier transform of the retarded Green function $G^r(\epsilon)$.[32] In terms of $A(\epsilon, t)$ the occupation $N(t)$ [using Eq. (31) for $G^<$] is given by

$$N(t) = \sum_{L,R} \Gamma^{L/R} \int \frac{d\epsilon}{2\pi} f_{L/R}(\epsilon) |A_{L/R}(\epsilon, t)|^2 . \quad (44)$$

We write the current as a sum of currents flowing out from the central region into the left (right) contact (see also Fig. 9), and currents flowing into the central region from the left (right) contact, $J_{L/R}(t) = J_{L/R}^{\mathrm{out}}(t) + J_{L/R}^{\mathrm{in}}(t)$:[33]

$$J_{L/R}^{\mathrm{out}}(t) = -\frac{e}{\hbar}\Gamma^{L/R}(t) N(t) \quad (45)$$

$$J_{L/R}^{\mathrm{in}}(t) = -\frac{e}{\hbar}\Gamma^{L/R} u_{L/R}(t) \int \frac{d\epsilon}{\pi} f_{L/R}(\epsilon)$$

$$\times \mathrm{Im}\{A_{L/R}(\epsilon, t)\} . \quad (46)$$

It is readily verified that these expressions coincide with Eq. (37) if all time-dependent quantities are replaced by constants.

Employing the same approach as in Sec. IV C, and provided that $u_L(t) = u_R(t) = u(t)$, we find that the time-averaged current in the WBL is given by

$$\langle J \rangle = -\frac{2e}{\hbar}\frac{\Gamma^L \Gamma^R}{\Gamma^L + \Gamma^R} \int \frac{d\epsilon}{2\pi} \mathrm{Im}\{f_L(\epsilon)\langle u(t) A_L(\epsilon, t)\rangle$$

$$-f_R(\epsilon)\langle u(t) A_R(\epsilon, t)\rangle\} . \quad (47)$$

Unlike the general case of Eq. (27), there is no restriction in the WBL that the time dependence be the same in the two leads. Equation (47) can, therefore, be used for the case of a time-dependent bias, where $\Delta_L(t)$ and $\Delta_R(t)$ will be different. It is interesting to note that the function of energy appearing in the time-averaged current is positive definite. In particular, as is shown in Appendix C,

$$-\langle \mathrm{Im}\{u_{L/R}(t) A_{L/R}(\epsilon, t)\}\rangle = \frac{\Gamma}{2}\langle |A_{L/R}(\epsilon, t)|^2\rangle . \quad (48)$$

One consequence of (48) is that if only the level is time dependent the average current cannot flow against the bias.

In the next two sections we consider specific examples for the time variation, which are relevant for experimental situations.

2. Response to harmonic modulation

Harmonic time modulation is probably the most commonly encountered example of time dependence. Here we treat the case when the contact and site energy levels vary as

$$\Delta_{L/R,0}(t) = \Delta_{L/R,0} \cos(\omega t). \quad (49)$$

It is easy to generalize the treatment to situations where the modulation frequencies and/or phases are different in different parts of the device. Assuming that the barrier heights do not depend on time ($u_{L/R} = 1$), and substituting (49) in the expression (43) for $A(\epsilon, t)$, one finds[34]

$$A_{L/R}(\epsilon, t) = \exp\left[-i\frac{(\Delta_0 - \Delta_{L/R})}{\omega}\sin(\omega t)\right]$$

$$\times \sum_{k=-\infty}^{\infty} J_k\left(\frac{\Delta_0 - \Delta_{L/R}}{\omega}\right)$$

$$\times \frac{e^{ik\omega t}}{\epsilon - \epsilon_0 - k\omega + i\Gamma/2} , \quad (50)$$

where $J_{-k}(x) = (-1)^k J_k(x)$. Figures 3(a) and (b) show $|A(\epsilon, t)|^2$ and $\mathrm{Im}A(\epsilon, t)$ as a function of time, respectively. We recall from Eqs. (44)–(45) that the current at a given time is determined by integrating $|A(\epsilon, t)|^2$ and $\mathrm{Im}A(\epsilon, t)$
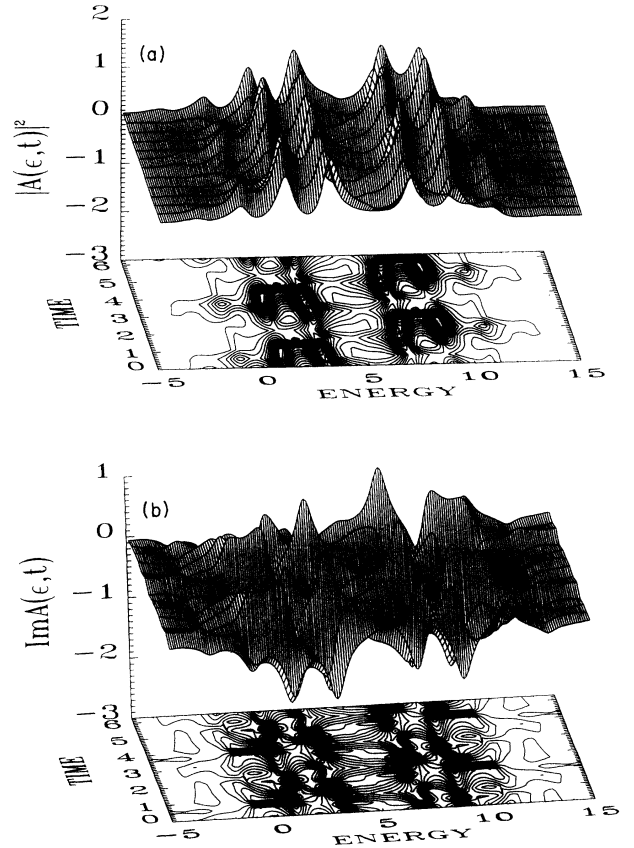

FIG. 3. (a) $|A(\epsilon, t)|^2$ as a function of time for harmonic modulation for a symmetric structure, $\Gamma_L = \Gamma_R = \Gamma/2$. The unit for the time axis is $\hbar/\Gamma$, and all energies are measured in units of Γ, with the values $\mu_L = 10$, $\mu_R = 0$, $\epsilon_0 = 5, \Delta = 5, \Delta_L = 10$, and $\Delta_R = 0$. The modulation frequency is $\omega = 2\Gamma/\hbar$. (b) The time dependence of $\mathrm{Im}A(\epsilon, t)$ for the case shown in (a).

over energy, and thus an examination of Fig. 3 helps to understand to complicated time dependence discussed below. (We show only A_L; similar results hold for A_R.) The physical parameters used to generate these plots are given in the figure caption. The three-dimensional plot (top part of figure) is projected down on a plane to yield a contour plot in order to help to visualize the time dependence. As expected, the time variation is periodic with period $T = 2\pi/\omega$. The time dependence is strikingly complex. The most easily recognized features are the maxima in the plot for $|A|^2$; these are related to photon sidebands occuring at $\epsilon = \epsilon_0 \pm k\omega$ [see also Eq. (51) below].[35]

The current is computed using the methods described in Appendix B, and is shown in Fig. 4. We also display the drive voltage as a broken line. Bearing in mind the complex time dependence of $|A|^2$ and ImA, which determine the out and in currents, respectively, it is not surprising that the current displays a nonadiabatic time dependence. The basic physical mechanism underlying the secondary maxima and minima in the current is the lineup of a photon-assisted resonant-tunneling peak with the contact chemical potentials. The rapid time variations are due to J^{in} (or, equivalently, due to ImA): the out-current J^{out} is determined by the occupation $N(t)$, and hence varies only on a time scale $\Gamma/\hbar$, which is the time scale for charge density changes.

We next consider the time average of the current. For the case of harmonic time dependence, we find[34]

$$\langle \text{Im}A_{L/R}(\epsilon,t) \rangle = -\frac{\Gamma}{2} \sum_{k=-\infty}^{\infty} J_k^2 \left(\frac{\Delta_0 - \Delta_{L/R}}{\omega} \right) \times \frac{1}{(\epsilon - \epsilon_0 - k\omega)^2 + (\Gamma/2)^2} . \tag{51}$$

Figure 5 shows the resulting time-averaged current J_{dc}. A consequence of the complex harmonic structure of the time-dependent current is that for temperatures $k_BT < \hbar\omega$ the average current oscillates as a function of period $2\pi/\omega$. The oscillation can be understood by examining the general expression for average current Eq. (27) together with (51): whenever a photon-assisted peak in the effective density of states, occuring at $\epsilon = \epsilon_0 \pm k\omega$ in the time-averaged density of states $\langle \text{Im}A_{L/R} \rangle$, moves in or out of the allowed energy range, determined by the difference of the contact occupation factors, a maximum (or minimum) in the average current results.

3. Response to steplike modulation

We give results for the case when the central site level changes abruptly at $t = t_0$: $\epsilon_0 \rightarrow \epsilon_0 + \Delta$. If the contacts also change at the same time, the corresponding results are obtained by letting $\Delta \rightarrow \Delta - \Delta_{L/R}$. Thus, simultaneous and equal shifts in the central region and the contacts have no effect. Assuming that the barrier heights do not depend on time ($u_{L/R} \equiv 1$), one finds for $t > t_0$ from Eq. (43)

$$A(\epsilon,t) = \frac{1}{\epsilon - \epsilon_0 + i\Gamma/2} \left\{ 1 + \Delta \frac{1 - \exp\left[i\{\epsilon - (\epsilon_0 + \Delta) + i\Gamma/2\}(t - t_0)\right]}{\epsilon - (\epsilon_0 + \Delta) + i\Gamma/2} \right\} . \tag{52}$$

This result is easily generalized [see Eq. (14) in Ref. 17] to a pulse of duration s, and numerical results are discussed below.

It is instructive to study analytically the long- and short-time behavior of $A(\epsilon,t)$. It easily verified that $A(\epsilon,t)$ has the expected limiting behavior
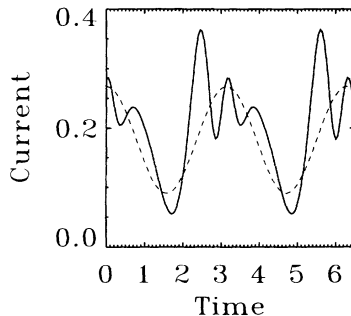

FIG. 4. The time-dependent current $J(t)$ for harmonic modulation corresponding to the parameters of Fig. 3. The dc bias is defined via $\mu_L = 10$ and $\mu_R = 0$, respectively. The dotted line shows (not drawn to scale) the time dependence of the drive signal. The temperature is $k_BT = 0.1\Gamma$.

$$A(\epsilon, t \rightarrow \infty) = [\epsilon - (\epsilon_0 + \Delta) + i\Gamma/2]^{-1} . \tag{53}$$

Thus, when the transients have died away, $A(\epsilon,t)$ settles to its new steady-state value.

Consider next the change in current at short times after the pulse, $t - t_0 \equiv \delta t \ll \hbar/\Gamma, \hbar/\epsilon$. Note that the second inequality provides an effective cutoff for the energy integration required for the current. In this limit we may write
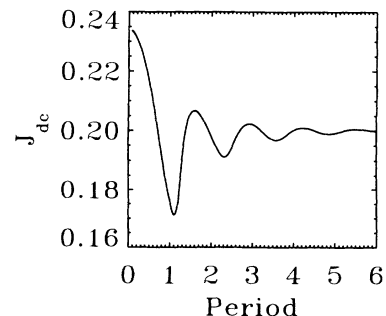

FIG. 5. Time-averaged current J_{dc} as function of the ac oscillation period $2\pi/\omega$. The dc amplitudes are the same as those in Fig. 4.

$$A(\epsilon, t) \simeq \frac{1 - i\Delta\delta t}{\epsilon - \epsilon_0 + i\Gamma/2}. \qquad (54)$$

Since $\delta J^{\mathrm{out}}(t) \propto |A(\epsilon, t)|^2 \propto (\delta t)^2$, the leading contribution comes from $J^{\mathrm{in}}(t)$. For low temperatures we find

$$\delta J_{L/R}(t) \simeq \frac{e\Gamma^{L/R}}{\pi\hbar} \int_{-\hbar/\delta t}^{\mu_{L/R}} d\epsilon \mathrm{Im}\delta A(\epsilon, t)$$

$$\simeq \frac{e\Gamma^{L/R}}{\pi\hbar} \Delta\delta t \ln \delta t. \qquad (55)$$

We next discuss the numerical results for a steplike modulation. Just like in the case of harmonic modulation, it is instructive to study the time dependence of $|A|^2$ and $\mathrm{Im}A$; these are shown in Figs. 6(a) and (b), respectively. The observed time dependence is less complex than in the harmonic case. Nevertheless, the resulting current, which we have computed for a pulse of duration s, and display in Fig. 7, shows an interesting ringing behavior. The ringing is again due to the movement of the sidebands of $\mathrm{Im}A_{L/R}$ through the contact Fermi energies.

Due to the experimental caveats discussed in Sec. II, the ringing shown in Fig. 7 may be masked by capacitive effects not included in the present work. However, the ringing should be observable in the time-averaged cur-
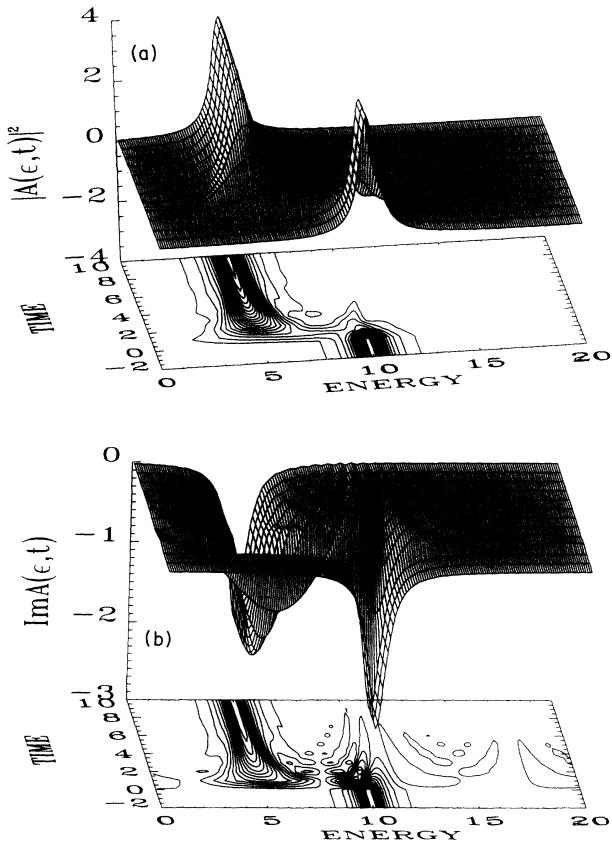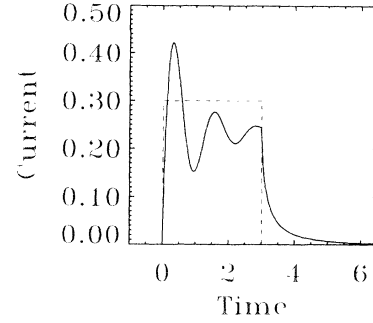

FIG. 7. Time-dependent current $J(t)$ through a symmetric double-barrier tunneling structure in response to a rectangular bias pulse. Initially, the chemical potentials μ_L and μ_R and the resonant-level energy ϵ_0 are all zero. At $t = 0$, a bias pulse (dashed curve) suddenly increases energies in the left lead by $\Delta_L = 10$ and increases the resonant-level energy by $\Delta = 5$. At $t = 3$, before the current has settled to a new steady value, the pulse ends and the current decays back to zero. The temperature is $k_B T = 0.1\Gamma$.

rent by applying a series of pulses such as that of Fig. 7, and then varying the pulse duration.[36] In Fig. 8 the derivative of the dc current with respect to pulse length is plotted, normalized by the repeat time τ between pulses. For pulse lengths s of the order of the resonance lifetime $\hbar/\Gamma$, the derivative of the dc current mimics closely the time-dependent current following the pulse, and, likewise, asymptotes to the steady-state current at the new voltage.

4. Linear response

For circuit modeling purposes it would often be desirable to replace the mesoscopic device with a conventional circuit element, with an associated complex impedance $Z(\omega)$, or admittance $Y(\omega)$. Our results for the nonlinear time-dependent current form a very practical starting point for such a calculation. For the noninteracting case, the current is determined by $A(\epsilon, t)$ [see Eqs. (44) and (45)], and all one has to do is to linearize A [Eq. (43)] with respect to the amplitude of the drive signal, i.e.,
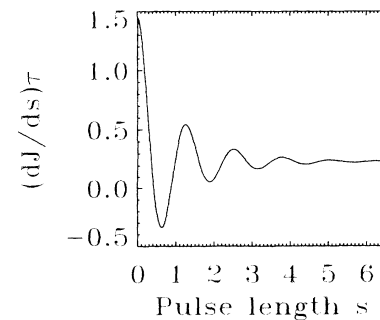

FIG. 6. (a) $|A(\epsilon, t)|^2$ as a function of time for steplike modulation. At $t = 0$ the resonant-level energy ϵ_0 suddenly decreases by 5Γ. (b) The time dependence of $\mathrm{Im}A(\epsilon, t)$ for the case shown in Fig. 6(a).

FIG. 8. Derivative of the integrated dc current J_{dc} with respect to pulse duration s, normalized by the interval between pulses τ. For pulse durations much longer than the resonance lifetime $\hbar/\Gamma$, the derivative is just the steady-state current at the bias voltage, but for shorter pulses the ringing response of the current is evident.

$\Delta - \Delta_{L/R}$. It is important to notice that we do not linearize with respect to the chemical potential difference: the results given below apply to an arbitrary static bias voltage.

Performing the linearization, one finds

$$|A^{(1)}_{L/R}(\epsilon, t)|^2 = \frac{\Delta - \Delta_{L/R}}{\omega} \mathrm{Re}\left\{ \frac{1}{\epsilon - \epsilon_0 + i\Gamma/2} \right.$$
$$\times \left[\frac{e^{-i\omega t}}{\epsilon - \epsilon_0 - \omega - i\Gamma/2} \right.$$
$$\left.\left. - \frac{e^{i\omega t}}{\epsilon - \epsilon_0 + \omega - i\Gamma/2} \right] \right\}, \qquad (56)$$

and

$$\mathrm{Im}A^{(1)}_{L/R}(\epsilon, t) = \frac{\Delta - \Delta_{L/R}}{2\omega} \mathrm{Im}\left\{ \frac{e^{i\omega t}}{\epsilon - \epsilon_0 - \omega + i\Gamma/2} \right.$$
$$\left. - \frac{e^{-i\omega t}}{\epsilon - \epsilon_0 + \omega + i\Gamma/2} + \frac{e^{-i\omega t} - e^{i\omega t}}{\epsilon - \epsilon_0 + i\Gamma/2} \right\}. \qquad (57)$$

At finite temperature the energy integration must be done numerically, as explained in Appendix B, while at $T = 0$ they can be done analytically. In the latter case, all the integrals can be cast into the form

$$\int_{-\infty}^{\mu} \frac{d\epsilon}{(\epsilon - \epsilon_1 + i\Gamma_1/2)(\epsilon - \epsilon_2 + i\Gamma_2/2)}$$
$$= \frac{1}{\epsilon_1 - \epsilon_2 + i(\Gamma_2 - \Gamma_1)/2} \ln \frac{\mu - \epsilon_1 + i\Gamma_1/2}{\mu - \epsilon_2 + i\Gamma_2/2}. \qquad (58)$$

Using

$$\ln(x + iy) = 1/2 \ln(x^2 + y^2) + i\tan^{-1}(y/x)$$

yields

$$J^{(1),\mathrm{in}}_{L/R} = \frac{e}{\hbar} \Gamma^{L/R} \frac{\Delta - \Delta_{L/R}}{2\pi\omega} [\cos(\omega t)F_{L/R}(\omega)$$
$$+ \sin(\omega t)G_{L/R}(\omega)] \qquad (59)$$

and

$$J^{(1),\mathrm{out}}_{L/R} = \frac{e}{\hbar} \Gamma^{L/R} \sum_{L,R} \Gamma^{L/R} \frac{\Delta - \Delta_{L/R}}{2\pi\omega} \left\{ \cos(\omega t)\left[\frac{\omega}{\omega^2 + \Gamma^2}G_{L/R}(\omega) - \frac{\Gamma}{\omega^2 + \Gamma^2}F_{L/R}(\omega) \right] \right.$$
$$\left. - \sin(\omega t)\left[\frac{\Gamma}{\omega^2 + \Gamma^2}G_{L/R}(\omega) + \frac{\omega}{\omega^2 + \Gamma^2}F_{L/R}(\omega) \right] \right\}, \qquad (60)$$

where we defined

$$G_{L/R}(\omega) = \ln \frac{|\mu_{L/R} - \epsilon_0 + i\Gamma/2|^2}{|(\mu_{L/R} - \epsilon_0 + i\Gamma/2)^2 - \omega^2|} \qquad (61)$$

and

$$F_{L/R}(\omega) = \tan^{-1}\frac{\mu_{L/R} - \epsilon_0 - \omega}{\Gamma/2}$$
$$- \tan^{-1}\frac{\mu_{L/R} - \epsilon_0 + \omega}{\Gamma/2}. \qquad (62)$$

These expressions give the linear ac current for an arbitrarily biased double barrier structure, where both contacts and the central-region energies are allowed to vary harmonically. As a check, it is instructive to verify that the finite temperature results of Appendix B 2 contain Eqs. (59) and (60) as a special case; this is a rather straightforward calculation using the limiting behavior of the Digamma function.

Considerable simplification occurs, if one considers a symmetric structure at zero bias: $\Gamma^L = \Gamma^R = \Gamma/2$, and $\mu_L = \mu_R \equiv \mu$, respectively. Following Fig. 9, the net current from left to right is

$$J^{(1)} = 1/2[J^{(1),\mathrm{in}}_L + J^{(1),\mathrm{out}}_R - J^{(1),\mathrm{out}}_L - J^{(1),\mathrm{in}}_R].$$

Using Eqs. (59) and (60), one finds that the "out" con-

tributions cancel, and that the "in" currents combine to give the net current

$$J^{(1)}(t) = -\frac{e}{\hbar} \frac{\Gamma}{4} \frac{\Delta_L - \Delta_R}{2\pi\omega} [\cos(\omega t)F(\omega) + \sin(\omega t)G(\omega)]. \qquad (63)$$

Here the functions $F(\omega)$ and $G(\omega)$ are given by Eqs. (62) and (61) but using μ and $\Gamma/2$ as parameters. This result exactly coincides with the recent calculation of Fu and Dudley,[21] which employed the ac Landauer-Büttiker linear-response theory.

We now wish to apply the formal results derived in this section to an experimentally relevant system. The
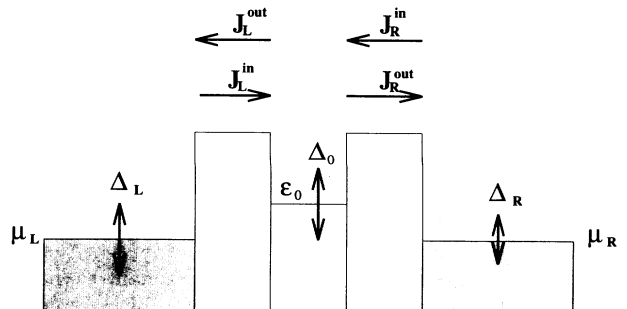

FIG. 9. Linear-response configuration.

archetypal mesoscopic device with potential for applications is the resonant-tunneling diode. The key feature of a resonant-tunneling diode is its ability to show negative differential resistance (NDR). The WBL model studied in this section does not have this feature: its I-V characteristic, which is readily evaluated with Eq. (37), is a monotonically increasing function. A much more interesting model can be constructed by considering a model where the contacts have a finite occupied bandwidth; this can be achieved by introducing a low energy cutoff $D_{L/R}$ (in addition to the upper cutoff provided by the electrochemical potential). The zero-temperature I-V characteristic is now

$$J_{dc}(V) = \frac{e}{h} \frac{2\Gamma_L \Gamma_R}{\Gamma} \left[\tan^{-1} \frac{\mu_L - \epsilon_0(V)}{\Gamma/2} \right.$$
$$- \tan^{-1} \frac{\mu_L - D_L - \epsilon_0(V)}{\Gamma/2}$$
$$- \tan^{-1} \frac{\mu_R(V) - \epsilon_0(V)}{\Gamma/2}$$
$$\left. + \tan^{-1} \frac{\mu_R(V) - D_R - \epsilon_0(V)}{\Gamma/2} \right] . \quad (64)$$

Here we assume that the right chemical potential is field dependent: $\mu_R(V) = \mu_R - eV$, and that the field dependence of the central-region level is given by $\epsilon_0(V) = \epsilon_0 - V/2$. The resulting current-voltage characteristic is depicted in Fig. 10. We note that the strong increase in current, which is observed in experimental systems at very high voltages, is not present in our model: this is because we have ignored the bias dependence of the barrier heights as well as any higher lying resonances. The only generalization required for Eqs. (59) and (60) is to modify the F and G functions: $F_\mu \to \tilde{F} = F_\mu - F_{\mu-D}$, and analogously for G_μ. We show in Fig. 11 the resulting linear-response admittance $Y(\omega)$ for a symmetric structure ($\Gamma_L = \Gamma_R$). Several points are worth noticing. For dc bias $eV = 5$ (energies are given in units of Γ) the calculated admittance resembles qualitatively the results reported by Fu and Dudley for zero external bias, except that the change in sign for the imaginary part of $Y(\omega)$ is not seen. For zero external bias (not shown in the figure) our finite bandwidth model leads to an admittance,
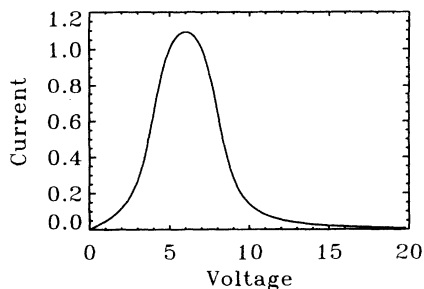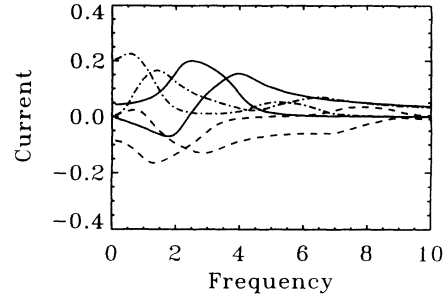

FIG. 11. In-phase and out-of-phase components of the linear-response current (in units of $e\Gamma/h$ and normalized with the amplitude of the drive signal Δ_L to yield admittance) for two bias points, $eV = 5$ (continuous line) and $eV = 10$ (dashed line). Other parameters are as in Fig. 10. The out-of-phase components (or, equivalently, imaginary parts) always tend to zero for vanishing frequency, while the in-phase component can have either a positive or negative zero-frequency limit depending on the dc bias.

whose imaginary part changes sign, and thus the behavior found by Fu and Dudley cannot be ascribed to an artefact of their infinite bandwidth model. More interestingly, for dc bias in the NDR regime, the real part is negative for small frequencies. This simply reflects the fact that the device is operating under NDR bias conditions. At higher frequencies the real part becomes positive, thus indicating that further modeling along the lines sketched here may lead to important implications on the high-frequency response of resonant-tunneling structures.

In concluding this section, we wish to emphasize that the linear-response analysis presented above is only a special case of the general results of Sec. IV, which seem to have the potential for many applications.

VI. RESONANT TUNNELING WITH ELECTRON-PHONON INTERACTIONS

As a final application, we establish a connection to previous calculations on the effect of phonons on resonant tunneling.[22] For simplicity, we consider a single resonant level with energy-independent level widths Γ_L and Γ_R (i.e., the WBL). The expression for the current Eq. (21) becomes now

$$J = \frac{e}{\hbar} \frac{\Gamma^L \Gamma^R}{\Gamma^L + \Gamma^R} \int \frac{d\epsilon}{2\pi} [f_L(\epsilon) - f_R(\epsilon)] \int_{-\infty}^{\infty} dt e^{i\epsilon t} a(t) , \quad (65)$$

where $a(t) = i[G^r(t) - G^a(t)]$ is the interacting spectral density. In general, an exact evaluation of $a(t)$ is not possible, however, if one ignores the Fermi sea, $G^r(t)$ [and hence $a(t)$] can be calculated exactly[37]

$$G^r(t) = -i\theta(t) \exp[-it(\epsilon_0 - \Delta) - \Phi(t) - \Gamma t/2] , \quad (66)$$

where

FIG. 10. I-V characteristic for a model resonant-tunneling device (quantum dot). The system is defined by parameters $\epsilon_0(V = 0) = 2$, $\mu_L = \mu_R(V = 0) = 0$, and $D_L = D_R = 2$, and the current is given in units of $e\Gamma/h$.

$$\Delta = \sum_{\mathbf{q}} \frac{M_{\mathbf{q}}^2}{\omega_{\mathbf{q}}} , \tag{67}$$

and

$$\Phi(t) = \sum_{\mathbf{q}} \frac{M_{\mathbf{q}}^2}{\omega_{\mathbf{q}}^2} [N_{\mathbf{q}}(1 - e^{i\omega_{\mathbf{q}}t}) + (N_{\mathbf{q}} + 1)(1 - e^{-i\omega_{\mathbf{q}}t})] ,$$

$$\tag{68}$$

and the electron-phonon interaction is given by Eq. (5). When substituted in the expression for current, one recovers the result of Ref. 22, which originally was derived by analyzing the much more complex two-particle Green function

$$G(\tau, s, t) = \theta(s)\theta(t)\langle d(\tau - s)d^\dagger(\tau)d(t)d^\dagger(0)\rangle.$$

The advantage of the method presented here is that one only needs the *single*-particle Green function to use the interacting current formula (21). Other systematic approaches to the single-particle Green function can, therefore, be directly applied to the current (e.g., perturbation theory in the tunneling Hamiltonian).

VII. CONCLUSIONS

Here, we summarize the main results of this study. We have derived a general formula for the time-dependent current through an interacting mesoscopic region, Eq. (15). The current is written in terms of local Green functions. This general expression is then examined in several special cases: (i) It is shown how earlier results for time-independent current are contained in it [Eqs. (19) and (21)]. (ii) An exact solution, for arbitrary time-dependence, for a single noninteracting level coupled to two leads is given [Eqs. (44) and (45)]. This calculation leads to a prediction of "ringing" of current in response to abrupt change of bias, or in response to an ac bias. We believe that this prediction should be experimentally verifiable. (iii) We derive a Landauer-like formula for the average current, Eq. (27). Finally, as applications, we discuss (iv) ac linear-response at arbitrary dc bias and finite temperature, and (v) find a connection to earlier results on resonant tunneling in the presence of optical phonons.

We hope that time dependence will provide a new window on coherent quantum transport, and will lead to significant new insights in the future.

ACKNOWLEDGMENTS

APPENDIX A: NONEQUILIBRIUM GREEN FUNCTIONS

The most important result (see, e.g., Refs. 25, 26, and 27) of the formal theory of nonequilibrium Green functions is that the perturbation expansion has precisely the *same structure* as the $T = 0$ equilibrium expansion. Instead of a time-ordered Green function, one works with the contour-ordered Green function,

$$G(\tau, \tau') = -i\langle T_C\{\psi(\tau)\psi^\dagger(\tau')\}\rangle , \tag{A1}$$

where the contour C is shown in Fig. 2. The contour-ordering operator T_C orders the operators following it in the contour sense: operators with time labels later on the contour are moved left of operators of earlier time labels. Thus, once the self-energy functional, $\Sigma = \Sigma[G]$, has been specified, the contour-ordered Green function obeys formally the same Dyson equation as in $T = 0$ theory,

$$G = G_0 + G_0 \Sigma G , \tag{A2}$$

with the modification that internal time integrations run along the (complex) path discussed in Sec. II A. It follows from this structural equivalence that one can derive equations of motion just as in the $T = 0$ case, and that the passage to nonequilibrium takes place by replacing the time-ordered Green functions by contour-ordered Green functions, and by replacing the real-time integration by an integration along the time contour. In practical calculations, however, the contour-ordered Green functions are inconvenient, and it is expedient to perform an analytic continuation to the real axis. The first step in this procedure consists of expressing the contour-ordered Green functions in terms of 2×2 matrices, whose elements are determined by which branches of the contour the two time labels are located on. The four elements of the matrix Green function are not linearly independent, and it is useful to perform a rotation of this matrix. A particularly convenient set of operational rules has been given by Langreth:[25] If one has an expression $A = \int BC$ on the contour (this is the generic type of term encountered in the perturbation expansion), then the retarded and lesser components are given by

$$A^r(t, t') = \int dt_1 B^r(t, t_1)C^r(t_1, t'),$$

$$A^<(t, t') = \int dt_1 [B^r(t, t_1)C^<(t_1, t')$$

$$+ B^<(t, t_1)C^a(t_1, t')]. \tag{A3}$$

These results are readily generalized to products involving three (or more) Green functions or self-energies.

The equation of motion for $G^<$ can be derived by applying the rules (A3) to the Dyson equation for the contour-ordered Green function. The Dyson equation can be written either in a differential form, or in an inte-

gral form, as in Eq. (A2). The former leads to the Baym-Kadanoff transport equation, while the latter (which is employed in the present work) yields the Keldysh equation for the lesser function

$$G^< = (1 + G^r \Sigma^r) G_0^< (1 + \Sigma^a G^a) + G^r \Sigma^< G^a , \quad \text{(A4)}$$

where the retarded and advanced Green functions satisfy

$$G^{r,a} = G_0^{r,a} + G_0^{r,a} \Sigma^{r,a} G^{r,a} . \quad \text{(A5)}$$

The physical modeling goes in the choice of the self-energy functional Σ, which contains the interactions (carrier-impurity scattering, phonon scattering, carrier-carrier scattering, etc.). Once Σ is given, for example in terms of diagrams, the retarded, or "lesser" components of the self-energy can be worked out according to the rules (A3), and one can proceed to solve the coupled Eqs. (A4) and (A5).

APPENDIX B: DYSON EQUATION FOR $G_{N,K\alpha}^t$

1. Equation-of-motion method

According to Appendix A it is sufficient to consider the $T = 0$ equation of motion for the time-ordered Green function $G_{n,k\alpha}^t$:

$$-i\frac{\partial}{\partial t'} G_{n,k\alpha}^t(t - t') = \epsilon_k G_{n,k\alpha}^t(t - t')$$
$$+ \sum_m V_{k\alpha,m}^* G_{nm}^t(t - t') , \quad \text{(B1)}$$

where we defined the central-region time-ordered Green function $G_{nm}^t(t - t') = -i\langle T\{d_m^\dagger(t')d_n(t)\}\rangle$. Note that it is crucial that the leads be noninteracting: had we allowed interactions in the leads the equation-of-motion technique would have generated higher order Green functions in Eq. (B1), and we would not have a closed set of equations.

We can interpret the factors multiplying $G_{n,k\alpha}^t(t - t')$ as the inverse of the contact Green-function operator, and introduce a short-hand notation: $G_{n,k\alpha}^t g_{k\alpha}^{-1} = \sum_m G_{nm}^t V_{k\alpha,m}^*$. By operating with $g_{k\alpha}^t$ from right, we arrive at

$$G_{n,k\alpha}^t(t - t') = \sum_m \int dt_1 G_{nm}^t(t - t_1)$$
$$\times V_{k\alpha,m}^* g_{k\alpha}^t(t_1 - t') . \quad \text{(B2)}$$

According to the rules of the nonequilibrium theory, this equation has in nonequilibrium precisely the same form, except that the intermediate time integration runs on the complex contour:

$$G_{n,k\alpha}(\tau, \tau') = \sum_m \int d\tau_1 G_{nm}(\tau, \tau_1)$$
$$\times V_{k\alpha,m}^*(\tau_1) g_{k\alpha}(\tau_1, \tau') . \quad \text{(B3)}$$

This is Eq. (11) of the main text. The analytic continu-

2. S-matrix expansion

We write the Green function $G_{n,k\alpha}(t,t')$ in terms of interaction-picture operators (denoted by a tilde) by invoking the S matrix:

$$G_{n,k\alpha}(\tau, \tau') = -i\langle T_C\{S\tilde{d}_n(\tau)\tilde{c}_{k\alpha}^\dagger(\tau')\}\rangle , \quad \text{(B4)}$$

where

$$S = T_C\left\{\exp\left[-i\int_C d\tau_1 \tilde{H}_T(\tau_1)\right]\right\} \quad \text{(B5)}$$

is the contour-ordered S matrix, and H_T is the tunneling Hamiltonian of Sec. II B 2. We expand the exponential function in (B5); the zeroth order term does not contribute, and we find

$$G_{n,k\alpha}(\tau, \tau') = -i\left\langle T_C\left\{ \tilde{d}_n(\tau)\tilde{c}_{k\alpha}^\dagger(\tau') \sum_{n=0}^\infty \frac{(-i)^{n+1}}{(n+1)!} \right.\right.$$
$$\times \left[\int_C d\tau_2 \sum_{k'\alpha',m} [V_{k'\alpha',m}(\tau_2) \right.$$
$$\times \tilde{c}_{k'\alpha'}^\dagger(\tau_2)\tilde{d}_m(\tau_2) + V_{k'\alpha',m}^*(\tau_2)$$
$$\left.\left.\left. \times \tilde{d}_m^\dagger(\tau_2)\tilde{c}_{k'\alpha'}(\tau_2)] \right]^{n+1} \right\}\right\rangle . \quad \text{(B6)}$$

Since, by assumption, the leads are noninteracting, result will only be nonzero if $\tilde{c}_{k\alpha}^\dagger(\tau')$ is contracted with $\tilde{c}_{k\alpha}(\tau_i)$ from one of the $n+1$ interaction terms. The $n+1$ possible choices cancels a factor of $n + 1$ in the factorial in the denominator, leaving

$$G_{n,k\alpha}(\tau, \tau') = \sum_m \int_C d\tau_2(-i)\langle T_C\{\tilde{c}_{k\alpha}(\tau_2)\tilde{c}_{k\alpha}^\dagger(\tau')\}\rangle$$
$$\times V_{k\alpha,m}^*(\tau_2)(-i)$$
$$\times \langle T_C\{S\tilde{d}_m^\dagger(\tau_2)\tilde{d}_n(\tau)\}\rangle . \quad \text{(B7)}$$

Equation (B7) is completely equivalent to the result (B3) obtained in the previous subsection.

APPENDIX C: PROOF OF EQ. (48)

In this Appendix, we prove that for a single level in the WBL (see Sec. V C) there is a definite relation,

$$-\langle u_{L/R}(t)\text{Im}\{A_{L/R}(\epsilon, t)\}\rangle = \frac{\Gamma}{2}\langle|A_{L/R}(\epsilon, t)|^2\rangle, \quad \text{(C1)}$$

between the time averages of the quantities that, respectively, determine the current and the occupation. For the case of the occupation, one can explicitly write out $\langle|A_{L/R}(\epsilon, t)|^2\rangle$ and then use the identity

$$G^r(t,t_1)G^a(t_1',t) = i\theta(t-t_1)\theta(t-t_1')$$
$$\times\left[e^{-\Gamma(t-t_1')}G^r(t_1',t_1)\right.$$
$$\left.-e^{-\Gamma(t-t_1)}G^a(t_1',t_1)\right] \qquad (C2)$$

to obtain

$$\langle|A|^2\rangle = \lim_{T\to\infty}\frac{i}{T\Gamma}\int_{-T/2}^{T/2}dt_1\int_{-T/2}^{T/2}dt_1'u_{L/R}(t_1)$$
$$\times u_{L/R}(t_1')[G^r(t_1',t_1) - G^a(t_1',t_1)]$$
$$\times\exp\left[i\epsilon(t_1'-t_1) + \int_{t_1}^{t_1'}dt_2\Delta(t_2)\right]. \qquad (C3)$$

Writing out $\langle u_{L/R}(t)\mathrm{Im}\{A_{L/R}(\epsilon,t)\}\rangle$ explicitly then yields Eq. (C1).

APPENDIX D: NUMERICAL INTEGRATION

In this Appendix, we describe methods to facilitate numerical calculations in the wide-band limit (Sec. V C). While the numerical integrations required for the occupation and for the current can be done directly, it is often difficult to obtain sufficient accuracy. We have found that it is useful to do the integrations analytically by contour integration, and then sum the resulting residues. We have also checked for a few selected parameter values that the two methods give identical results.

1. Steplike modulation

We illustrate the somewhat cumbersome but straightforward formulas by giving the expressions for the deviation of the occupation from its asymptotic value following a steplike modulation of the level energy (Sec. V C 3): $\delta N(t) = N(t) - N(t = \infty)$. We find from Eqs. (44) and (52)

$$\delta N(t) = \frac{1}{2\pi}\Delta^2 e^{-\Gamma(t-t_0)}[\Gamma^L D(\mu_L) + \Gamma^R D(\mu_R)]$$
$$-\frac{1}{2\pi}\Delta e^{-\Gamma(t-t_0)/2}[\Gamma^L 2\mathrm{Re}\{E(\mu_L)\}$$
$$+\Gamma^R 2\mathrm{Re}\{E(\mu_R)\}], \qquad (D1)$$

where

$$D(\mu) = \int d\epsilon\frac{f(\epsilon)}{(\epsilon-\epsilon_0-\Delta)^2 + (\Gamma/2)^2}\frac{1}{(\epsilon-\epsilon_0)^2 + (\Gamma/2)^2},$$

$$E(\mu) = \int d\epsilon\left[\frac{f(\epsilon)}{(\epsilon-\epsilon_0-\Delta)^2 + (\Gamma/2)^2}\right.$$
$$\left.\times\frac{e^{i(\epsilon-\epsilon_0-\Delta)(t-t_0)}}{\epsilon-\epsilon_0-i\Gamma/2}\right], \qquad (D2)$$

where $f(\epsilon)$ is the Fermi function with chemical potential μ. The poles of the integrands are at $\epsilon = \epsilon_0 \pm i\Gamma/2$, $\epsilon = \epsilon_0 + \Delta \pm i\Gamma/2$, and $\epsilon = \mu \pm i2\pi(n+1/2)/\beta$, respectively. Upon closing the contour in the upper-half plane, one obtains three different contributions; the terms aris-

ing from $\epsilon = \epsilon_0 + i\Gamma/2$ and $\epsilon = \epsilon_0 + \Delta + i\gamma/2$ obviously lead to no problems, while the sum over n converges either as n^{-4} [the term originating from $D(\mu)$], or as $n^{-3}\exp[-2\pi n(t-t_0)/\beta]$ [the term due to $E(\mu)$], and hence also converges rapidly.

2. Harmonic modulation

In principle, the calculation proceeds as in the previous section. However, the sum over the residues, which results from the contour integration, converges very slowly. A typical term in the resulting lengthy expressions converges only as n^{-2}. Significantly improved convergence can be obtained by making use of the relation

$$\sum_{n=0}^{\infty}\frac{1}{(n+a)(n+b)} = \frac{1}{a-b}[\Psi(a) - \Psi(b)], \qquad (D3)$$

where Ψ is the digamma function. In what follows, we give the results for *linear response*. The occupation [which also gives the current flowing out from the central region via (44)] is

$$N(t) = \frac{1}{2\pi}\sum_{L,R}\frac{\Delta_0 - \Delta_{L/R}}{\omega^2 + \Gamma^2}\frac{\Gamma^{L/R}}{\omega}\left\{\sin(\omega t)\left[2\Gamma r_0^{L/R}\right.\right.$$
$$+\omega(I_+^{L/R} - I_-^{L/R}) - \Gamma(R_+^{L/R} + R_-^{L/R})]$$
$$+\cos(\omega t)\left[-2\omega r_0^{R/L} + \omega(R_+^{L/R} + R_-^{R/L})\right.$$
$$\left.\left.+\Gamma(I_+^{L/R} - I_-^{L/R})\right]\right\}. \qquad (D4)$$

Here

$$I_\pm^{L/R} = \mathrm{Im}\left[\Psi\left(1/2 - \frac{\beta}{2\pi i}(\mu_{L/R} - \epsilon_0 \mp \omega - i\Gamma/2)\right)\right],$$

$$R_\pm^{L/R} = \mathrm{Re}\left[\Psi\left(1/2 - \frac{\beta}{2\pi i}(\mu_{L/R} - \epsilon_0 \mp \omega - i\Gamma/2)\right)\right],$$

$$r_0^{L/R} = \mathrm{Re}\left[\Psi\left(1/2 + \frac{\beta}{2\pi i}(\mu_{L/R} - \epsilon_0 + i\Gamma/2)\right)\right]. \qquad (D5)$$

The current flowing into the central region can also be expressed in terms of similar functions:

$$J_{L/R}^{\mathrm{in}}(t) = \frac{e}{\hbar}\Gamma^{L/R}\frac{\Delta - \Delta_{L/R}}{2\pi\omega}\left[\cos(\omega t)(i_-^{L/R} - i_+^{L/R})\right.$$
$$\left.+\sin(\omega t)(2r_0^{L/R} - r_+^{L/R} - r_-^{L/R})\right], \qquad (D6)$$

with

$$i_\pm^{L/R} = \mathrm{Im}\left[\Psi\left(1/2 + \frac{\beta}{2\pi i}(\mu_{L/R} - \epsilon_0 \mp \omega + i\Gamma/2)\right)\right],$$

$$r_\pm^{L/R} = \mathrm{Re}\left[\Psi\left(1/2 + \frac{\beta}{2\pi i}(\mu_{L/R} - \epsilon_0 \mp \omega + i\Gamma/2)\right)\right]. \qquad (D7)$$

By recalling $\lim_{z\to\infty}\Psi(z) \to \ln(z)$, it is straightforward to check that these results reduce to the $T = 0$ case discussed in the main text.

[1] For a series of review articles see, *Mesoscopic Phenomena in Solids*, edited by B.L. Altshuler, P.A. Lee, and R.A. Webb (Elsevier, Amsterdam, 1991).

[2] For a review see, P.A. Lee and T.V. Ramakrishnan, Rev. Mod. Phys. **57**, 287 (1985).

[3] Recent experimental advances are described, e.g., in *Nano-structures and Mesoscopic Systems*, edited by W.P. Kirk and M.A. Reed (Academic Press, San Diego, 1992); and *Proceedings of the 21st International Conference on the Physics of Semiconductors*, edited by P. Jiang and H-Z Zheng (World Scientific, Singapore, 1992).

[4] L.P. Kadanoff and G. Baym, *Quantum Statistical Mechanics* (Benjamin, New York, 1962).

[5] L.V. Keldysh, Zh. Eksp. Teor. Fiz. **47**, 1515 (1964) [Sov. Phys. JETP **20**, 1018 (1965)].

[6] An early reference to tunneling problems vs nonequilibrium Green functions is the series of papers by Caroli *et al.*; C. Caroli, R. Combescot, P. Nozieres, and D. Saint-James, J. Phys. C **4**, 916 (1971); C. Caroli, R. Combescot, D. Lederer, P. Nozieres, and D. Saint-James, *ibid.* **4**, 2598 (1971); R. Combescot, *ibid.* **4**, 2611 (1971); C. Caroli, R. Combescot, P. Nozieres, and D. Saint-James, *ibid.* **5**, 21 (1972).

[7] Y. Meir and N.S. Wingreen, Phys. Rev. Lett. **68**, 2512 (1992).

[8] J.H. Davies, S. Hershfield, P. Hyldgaard, and J.W. Wilkins, Phys. Rev. B **47**, 4603 (1993).

[9] E.V. Anda and F. Flores, J. Phys. Condens. Matter **3**, 9087 (1991).

[10] S. Hershfield, J.H. Davies, and J.W. Wilkins, Phys. Rev. Lett. **67**, 3720 (1991).

[11] Y. Meir, N.S. Wingreen, and P.A. Lee, Phys. Rev. Lett. **70**, 2601 (1993).

[12] R. Lake and S. Datta, Phys. Rev. B **45**, 6670 (1992).

[13] R. Landauer, IBM J. Res. Dev. **1**, 233 (1957); Philos. Mag. **21**, 863 (1970).

[14] A. Blandin, A. Nourtier, and D.W. Hone, J. de Physique **37**, 369 (1976).

[15] L.Y. Chen and C.S. Ting, Phys. Rev. B **43**, 2097 (1991).

[16] D.C. Langreth and P. Nordlander, Phys. Rev. B **43**, 2541 (1991).

[17] N.S. Wingreen, A.P. Jauho, and Y. Meir, Phys. Rev. B **48**, 8487 (1993).

[18] C. Bruder and H. Schoeller, Phys. Rev. Lett. **72**, 1076 (1994).

[19] E. Runge and H. Ehrenreich, Ann. Phys. (N.Y.) **219**, 55 (1992); Phys. Rev. B **45**, 9145 (1992).

[20] H.M. Pastawski, Phys. Rev. B **46**, 4053 (1992).

[21] Y. Fu and S.C. Dudley, Phys. Rev. Lett. **70**, 65 (1993).

[22] N.S. Wingreen, K.W. Jacobsen, and J.W. Wilkins, Phys. Rev. B **40**, 11834 (1989); see also, L.I. Glazman and R.I. Shekter, Zh. Eksp. Teor. Fiz. **94**, 292 (1987). [Sov. Phys. JETP **67**, 163 (1988)].

[23] A similar approach has recently been suggested by M. Büttiker, A. Prêtre, and H. Thomas, Phys. Rev. Lett. **70**, 4114 (1993).

[24] E.R. Brown *et al.*, Appl. Phys. Lett. **58**, 2291 (1991).

[25] D.C. Langreth, in *Linear and Nonlinear Electron Transport in Solids*, Vol. 17 of *Nato Advanced Study Institute, Series B: Physics*, edited by J.T. Devreese and V.E. Van Doren (Plenum, New York, 1976).

[26] J. Rammer and H. Smith, Rev. Mod. Phys. **58**, 323 (1986).

[27] A.P. Jauho, Solid State Electron. **32**, 1265 (1989).

[28] J. Schwinger, J. Math. Phys. **2**, 407 (1961); P.C. Martin and J. Schwinger, Phys. Rev. **115**, 1342 (1959).

[29] R. Lake, G. Klimeck, M.P. Anantram, and S. Datta, Phys. Rev. B **48**, 15132 (1993); see also R. Landauer, Phys. Scr. **T42**, 110 (1992).

[30] Note that the first term in (A4) is zero, because $[1 + G^r \Sigma^r] G_0^< = G^r (G_0^r)^{-1} G_0^< = 0$.

[31] T. Weil and B. Vinter, Appl. Phys. Lett. **50**, 1281 (1987); M. Jonson and A. Grincwajg, *ibid.* **51**, 1729 (1987).

[32] A remark about the notation: the reader should not confuse A with a (generalized) spectral function (which is also often denoted by A). We employ the symbol a for the spectral function, i.e., $a(\epsilon) = -2 \, \text{Im} \, G^r(\epsilon)$.

[33] The reader may worry about the direction of the in and out currents, because both terms in (45) apparently have the same sign. However, $\langle \text{Im} A \rangle < 0$ (See Appendix D for an explicit demonstration), and the in and out currents flow in opposite directions, as expected.

[34] It is useful to recall the identity $\exp[i\alpha \sin(\omega t)] = \sum_{k=-\infty}^{\infty} e^{i\omega t k} J_k(\alpha)$, where J_k is the kth order Bessel function.

[35] M. Büttiker and R. Landauer, Phys. Rev. Lett. **49**, 1739 (1982); Phys. Scr. **32**, 429 (1985).

[36] Leo Kouwenhoven (private communication).

[37] See, e.g., G.D. Mahan, *Many-Particle Physics*, 2nd ed. (Plenum Press, New York, 1990), pp. 285–324.

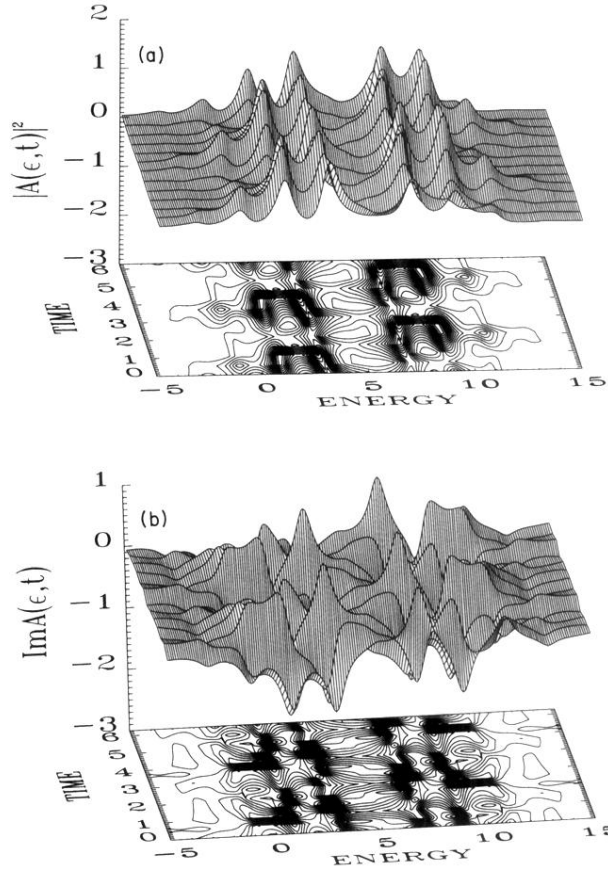[38] C. Jacoboni and P.J. Price, Solid State Commun. **75**, 193 (1990).

FIG. 3. (a) $|A(\epsilon, t)|^2$ as a function of time for harmonic modulation for a symmetric structure, $\Gamma_L = \Gamma_R = \Gamma/2$. The unit for the time axis is $\hbar/\Gamma$, and all energies are measured in units of Γ, with the values $\mu_L = 10$, $\mu_R = 0$, $\epsilon_0 = 5, \Delta = 5, \Delta_L = 10$, and $\Delta_R = 0$. The modulation frequency is $\omega = 2\Gamma/\hbar$. (b) The time dependence of $\text{Im}A(\epsilon, t)$ for the case shown in (a).
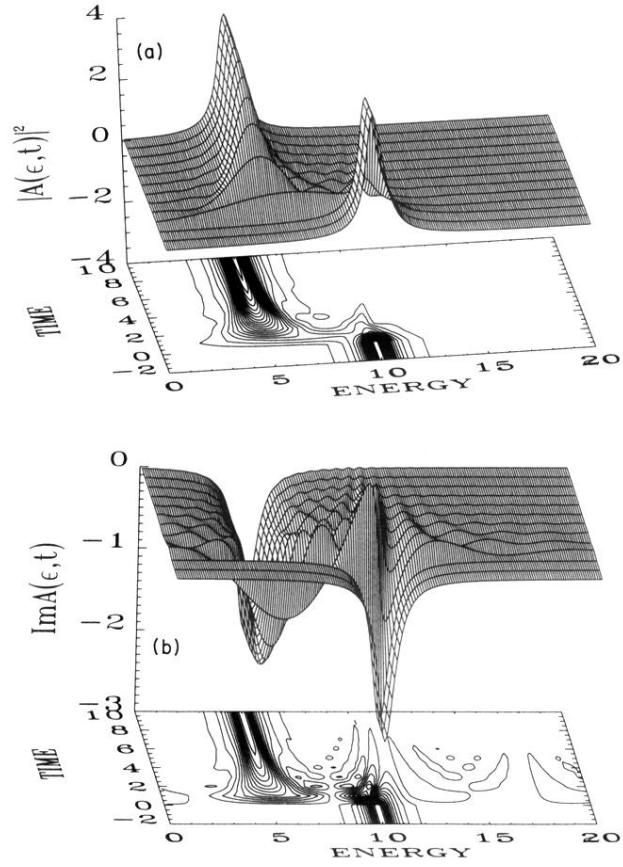
FIG. 6. (a) $|A(\epsilon, t)|^2$ as a function of time for steplike modulation. At $t = 0$ the resonant-level energy ϵ_0 suddenly decreases by 5Γ. (b) The time dependence of $\mathrm{Im}A(\epsilon, t)$ for the case shown in Fig. 6(a).
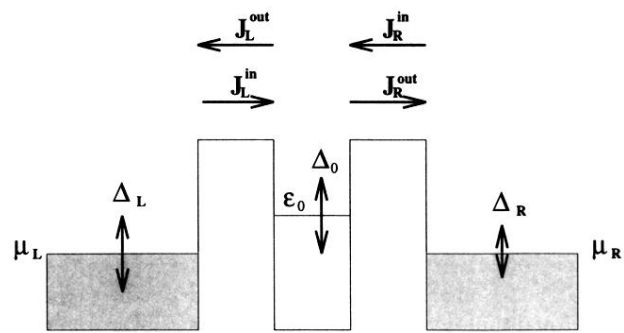
FIG. 9. Linear-response configuration.